NJC

LETTER

View Article Online
View Journal | View Issue

Cite this: *New J. Chem.*, 2016, **40**, 8206

Received (in Montpellier, France) 13th June 2016,
Accepted 8th August 2016

DOI: 10.1039/c6nj01854h

www.rsc.org/njc

Structural tailoring of the NIR-absorption of bis(1,2-dichalcogenolene) Ni/Pt electrochromophores deriving from 1,3-dimethyl-2-chalcogenoxo-imidazoline-4,5-dichalcogenolates†

Carlo Deiana,[a] M. Carla Aragoni,[a] Francesco Isaia,[a] Vito Lippolis,[a] Anna Pintus,[a] Alexandra M. Z. Slawin,[b] J. Derek Woollins[b] and Massimiliano Arca*[a]

The choice of the metal ion M and the terminal Y and donor X chalcogen species (M = Ni, Pt; and X, Y = S, Se) in square-planar complexes deriving from 1,3-dimethyl-2-chalcogenoxo-imidazoline-4,5-dichalcogenolates allows fine-tuning of both the redox stability and the energy of the particularly intense NIR electrochromic absorption, thanks to the subtle contribution of M, X, and Y to the relevant frontier molecular orbitals, investigated at the IEF-PCM DFT and TD-DFT level.

During the past few decades, the scientific community has been increasingly interested in bis(1,2-dithiolene) metal complexes,[1–3] largely because of their numerous fields of applications, ranging from optics,[2,4–7] to laser Q-switching and mode-locking,[5,8,9] and conductivity,[10–13] and due to their role in biochemistry.[14–17] A high degree of π-electron delocalization involves both the organic framework and the metal center, conferring d^8 metal ion bis(1,2-dithiolene) complexes specific molecular properties, such as planarity and the ability to carry a molecular charge[18] that can vary reversibly between −2 and +2, also assuming fractional values in non-integral oxidation state (NIOS) salts.[13] In this context, some of the authors have reported the class of bis(1,2-dithiolene) complexes $[M(R_2timdt)_2]^{x-}$ (M = Ni, Pd, Pt; R_2timdt^{2-} = 1,3-disubstituted 2-thioxoimidazoline-4,5-dithiolate; x = 0, 1, 2; Scheme 1),[19] which have been investigated as materials for nonlinear optical (NLO) applications,[9,20,21] photoconductors,[22,23] and, very recently, as highly efficient photothermal converters.[24] All these applications are related to the peculiar near infrared (NIR) absorption of neutral and radical monoanionic species,[19,22,24,25] attributed to a π–π* HOMO–LUMO and a SOMO–LUMO electron transition,[22] respectively, and falling between 990 and 1070 nm for the neutral $[M(R_2timdt)_2]$ species,[25] in the range of 1375–1745 nm for $[M(R_2timdt)_2]^-$ monoanions,[22] while dianions do not show any electronic absorption in the VIS-NIR region (M = Ni, Pd, Pt).

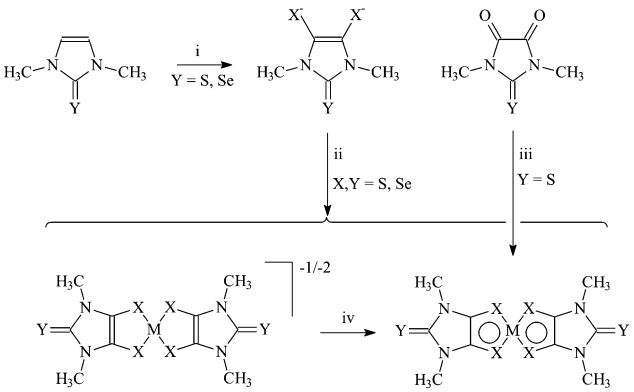

Scheme 1 Synthetic pathway for the preparation of complexes **1–8**. (i) THF, −10 °C, LDA, S/Se; (ii) THF, $NiCl_2{\cdot}6H_2O/K_2PtCl_4$, Et_4NI; (iii) refluxing toluene, Lawesson's reagent, Ni powder or $PtCl_2$, EtOH after concentration; and (iv) CH_2Cl_2, r.t., I_2. See the ESI† for details.

Surprisingly, bis(1,2-diselenolene) metal complexes have been explored much less[26] and a limited number of papers have been published on the optical properties of the corresponding homodileptic complexes.[3] This notwithstanding, the comparison of the absorption energy of the tetraethylammonium salts of the $[Ni(Me\text{-}dmet)_2]^-$ and $[Ni(Me\text{-}dmes)_2]^-$ monoanions (Me-$dmet^{2-}$ = *N*-methyl-2-thioxoimidazoline-4,5-dithiolate;[27] Me-$dmes^{2-}$ = *N*-methyl-2-thioxoimidazoline-4,5-diselenolate; λ_{max} = 1284 and 1187 nm, respectively, in CH_2Cl_2) clearly shows that the replacement of sulfur with selenium donor atoms affects the energy of the π–π* absorption band.[28] In addition, the nature of the terminal chalcogen atoms was shown to strongly affect the position of the NIR absorption band of the $[M(H_2timdt)_2]$ model dithiolenes (M = Ni, Pd, Pt).[29] While $[M(Me_2timdt)_2]$ complexes (M = Ni, **1**; Pt, **2**) could be prepared successfully by the reaction of the corresponding 2-thioxoimidazolidine-4,5-dione using Lawesson's

[a] *Dipartimento di Scienze Chimiche e Geologiche, Università degli Studi di Cagliari, S.S. 554 bivio per Sestu, 09042 Monserrato, Italy. E-mail: marca@unica.it*
[b] *EaStCHEM School of Chemistry, University of St. Andrews, North Haugh, St. Andrews, Fife, KY16 9ST, UK*

† Electronic supplementary information (ESI) available: Crystallographic data for **9**, NIR spectrophotometric and DFT/TD-DFT data. CCDC 1484547. For ESI and crystallographic data in CIF or other electronic format see DOI: 10.1039/c6nj01854h

Table 1 NIR absorption maxima λ_{max} (nm) and DFT-calculated reduction potential $E_{1/2}^{298K}$ (V *vs.* F_c^+/F_c) for compounds $(Et_4N)_n$[**1–8**] in CH_2Cl_2 (n = 0, 1)[a]

	M	X	Y	Ligand	$E_{1/2}^{298K}$	λ_{max} n = 0	λ_{max} n = 1
$\mathbf{1}^{n-}$	Ni	S	S	Me_2timdt^{2-}	−0.31	995	1438
$\mathbf{2}^{n-}$	Pt	S	S		−0.47	988	—[b]
$\mathbf{3}^{n-}$	Ni	S	Se	Me_2simdt^{2-}	−0.29	1065	1428
$\mathbf{4}^{n-}$	Pt	S	Se		−0.22	1006	1412
$\mathbf{5}^{n-}$	Ni	Se	S	Me_2timds^{2-}	−0.20	1097	1398
$\mathbf{6}^{n-}$	Pt	Se	S		−0.43	1054	1389
$\mathbf{7}^{n-}$	Ni	Se	Se	Me_2simds^{2-}	−0.09	—[c]	1399
$\mathbf{8}^{n-}$	Pt	Se	Se		−0.14	—[c]	1363

[a] X and Y chalcogen atoms as in Scheme 1. [b] The absorption band of the monoanion was not found in the NIR spectrum of the reaction product. [c] Diiodine oxidation did not succeed in generating the relevant neutral species.

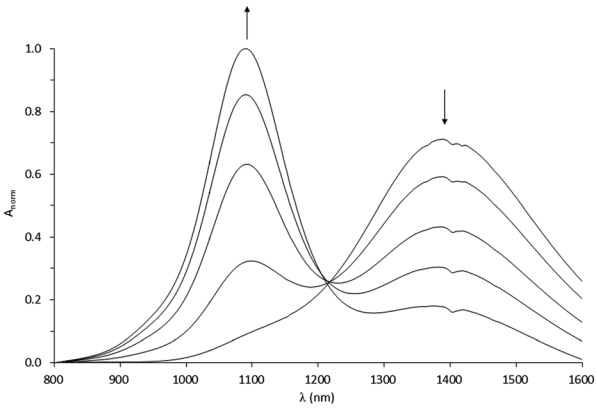

Fig. 1 Spectrophotometric titration of (Et_4N)(**5**) (λ_{max} = 1398 nm) with diiodine to give **5** (λ_{max} = 1097 nm) in CH_2Cl_2 solution.

reagent (LR; 2,4-bis(4-methoxyphenyl)-1,3,2,4-dithiadiphosphetane-2,4-disulfide;[30] synthetic pathway iii in Scheme 1),[19,25] any attempt at thiation of 2-selenoxo-imidazolidine-4,5-dione[31] using LR or selenation with Woollins' reagent (2,4-diphenyl-1,3,2,4-diselenadiphosphetan-2,4-diselenide)[32] in the presence of metal powder or salts failed. On the contrary, we succeeded in the preparation of the desired Ni and Pt complexes **1–8** by reacting the relevant metal salts ($NiCl_2{\cdot}6H_2O$ and K_2PtCl_4, respectively) with the Me_2timdt^{2-}, Me_2simdt^{2-}, Me_2timds^{2-}, and Me_2simds^{2-} ligands (Table 1). The ligands were generated *in situ* from the corresponding 1,3-dimethyl-2-chalcogenoxoimidazol-4,5-dichalcogenato precursors (pathway ii in Scheme 1), in turn obtained by the reaction of 1,3-dimethyl-2-chalcogenoxoimidazole with LDA followed by the desired chalcogen X (reaction i in Scheme 1).[33,34] Since in solution, even in the absence of air and light, a spontaneous degradation was clearly detectable using NIR spectroscopy, no electrochemical measurements could be carried out. NIR absorption spectroscopy in CH_2Cl_2 solution showed that the crude reaction products contain a mixture of the monoanionic and neutral complexes (absorbing in the range of 988–1097 and 1363–1438 nm, respectively), in ratios depending on the nature of the donor and terminal chalcogen atomic species. The absorption wavelength displayed by the neutral species was successfully measured by recording the UV-Vis-NIR spectrum of CH_2Cl_2 solutions after quantitative diiodine oxidation (reaction iv in Scheme 1; Fig. 1 and Fig. S1, S2 in the ESI† for **5** and $\mathbf{5}^-$), while in the case of the complexes deriving from the Me_2simds^{2-} ligand it was not possible to identify spectroscopically the neutral species (Fig. S3 in the ESI† for $\mathbf{7}^-$). On the whole, Ni and Pt homologues display very similar absorption energies, the Pt complexes featuring slightly lower λ_{max} values (Fig. S4 and S5, ESI†) as compared to Ni ones, in agreement with what was observed for $[Ni(Me\text{-}dmet)_2]^-$ and $[Ni(Me\text{-}dmes)_2]^-$.[28] Upon passing from $[M(Me_2timdt)_2]$ complexes to $[M(Me_2simdt)_2]$ and the $[M(Me_2simds)_2]$ species, a bathochromic shift of the absorption of the neutral species and hypsochromic shifts of the monoanions are observed (Fig. S5 in the ESI†), thus reducing the difference $\Delta\lambda^{-1/0}$ in the absorption wavelengths of the two differently charged species (Table S1 in the ESI†).‡ An interpretation of the spectroscopic features was achieved by means of theoretical calculations carried out at the density functional theory (DFT)[35] level. As a benchmark of the computational set-up (see the ESI†), the metric parameters optimized for **1** and **2** were found to be in an excellent agreement with the corresponding structural bond lengths and angles reported previously for $[Ni(R_2timdt)_2]$ complexes and $[Pt(Et_2timdt)_2]$ (**9**, Fig. 2; Table S3 in the ESI†), the first example of a Pt member of the $[M(R_2timdt)_2]$ series characterized structurally (Fig. S7 and Table S11 in the ESI†).§ Kohn-Sham (KS) HOMO (b_{1u}) and KS-LUMO (b_{2g}) in the ^1A_g ground state (GS)¶ are π and π*-in-nature molecular orbitals, respectively, involving mainly the np_z atomic orbitals (AOs) of the four chalcogen donor atoms X and four carbon atoms of the 1,2-dichalcogenolene system, along with the np_z AOs of the terminal chalcogen atoms Y (the symmetry labels refer to the molecule belonging to the D_{2h} point group and lying on the xy plane; n = 2, 3, and 4 for C, S, and Se, respectively). The central metal ion AOs are not involved in the KS-HOMO (0–2%), and only marginally in the KS-LUMO, with contributions that increase upon passing from Ni (4–5%) to Pt (8%) complexes (Table S14 in the ESI†). The contribution of atoms X to KS-HOMO and KS-LUMO is

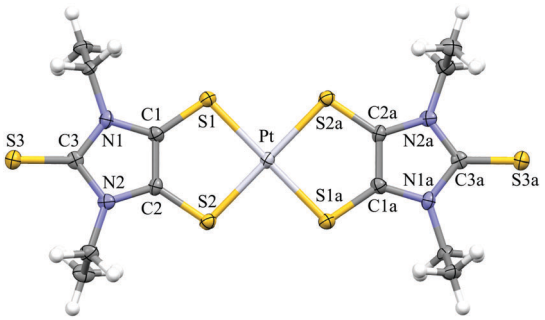

Fig. 2 Molecular view of complex **9**. Ellipsoids are drawn at the 60% probability level. Hydrogen atoms are shown as fixed-size spheres (radius 0.20 Å). Selected bond lengths and angles: Pt–S1, 2.2825(15); Pt–S2, 2.2825(15); C1–C2, 1.386(7); C1–S1, 1.687(5); C2-S2, 1.693(5); C1–N1, 1.687(5); C2–N2, 1.693(5); C3–N1, 1.369(7); C3–N2, 1.393(6); C3–S3, 1.660(5) Å; S1–Pt–S2, 91.89(5); S1–Pt–S2a, 88.11(5); C1–C2–S2, 123.9(4); C2–C1–S1, 124.5(4); C1–S1–Pt, 99.88(16); C2–S2–Pt, 99.8(2); N1–C1–C2, 106.6(4); N2–C2–C1, 107.7(4); C1–N1–C3, 110.8(4); C2–N2–C3, 109.4(4); N1–C3–N2, 105.6(4); N1–C3–S3, 127.1(4); N2–C3–S3, 127.4(1)°. a = 2 − x, −y, 1 − z. See Tables S3–S11 in the ESI† for further details.

independent of the nature of the chalcogen (about 6% and 12%, respectively, for each atom), while the contribution of the terminal atoms Y is larger when Y = Se (up to 21%) as compared to Y = S. Therefore, the replacement of S with Se results in a slight but progressive stabilization of KS-HOMO and to a lesser extent LUMO upon passing from **1** to **8** (Table S13 and Fig. S8 in the ESI†), in agreement with the increase of stability of the monoanionic species observed along the series (Fig. S9 in the ESI†). In the monoanionic species ($^2B_{2g}$ GS), the extra α-electron occupies the ligand centered b_{2g} π*-MO (Fig. S10 for **1** and $\mathbf{1}^-$, ESI†), thus decreasing the C–X bond orders and increasing those of C–C bonds, as testified by the structural and calculated metric parameter data (Tables S11 and S15 in the ESI†), while not affecting the oxidation state of the metal center, whose electron population was calculated at the NBO level to vary by less than 0.05 |e| upon passing from the neutral to monoanionic species. According to TD-DFT calculations, the peculiar intense spin-allowed NIR transition ($^1A_g \rightarrow {}^1B_{3u}$ and $^2B_{2g} \rightarrow {}^2B_{3u}$ for **1–8** and $\mathbf{1}^-$–$\mathbf{8}^-$, respectively) is largely ascribable to the HOMO → LUMO (85–90%) and HOMO → SOMO (98–100%) monoelectronic excitations ($b_{1u} \rightarrow b_{2g}$) for neutral and monoanionic species, respectively (Fig. S10; Tables S16 and S17 in the ESI†).¶ Implicit solvation is essential in evaluating correctly the transition energies, calculated in CH_2Cl_2 in the range of 1.19–1.26 and 0.80–0.92 eV for the neutral species and monoanions, respectively, with a good correlation ($R^2 = 0.94$) between experimental NIR λ_{max} values (Table 1) and the corresponding absorption maxima calculated at the TD-DFT level (Table S16, ESI†). Moreover, IEF-PCM TD-DFT calculations are in agreement with NIR spectroscopy data in indicating that the absorption wavelength difference $\Delta\lambda^{-1/0}$ between the NIR transitions peculiar to neutral and monoanionic complexes decreases along the series $Me_2timdt^{2-} < Me_2simdt^{2-} < Me_2timds^{2-} <$ and Me_2simds^{2-} (Table S16, ESI†). This is mainly due to the stabilization in HOMO eigenvalues of $\mathbf{1}^-$–$\mathbf{8}^-$, resulting in a HOMO–SOMO gap which passes from about 1.34 in $\mathbf{1}^-$ to 1.40 eV in $\mathbf{7}^-$ and from 1.46 in $\mathbf{2}^-$ to 1.51 eV in $\mathbf{8}^-$ in CH_2Cl_2 (Table S16, ESI†). An examination of the KS-MOs composition (Table S14, ESI†) clearly shows that the stabilization of the KS-HOMO in monoanions is due to the increasing participation of the np_z AOs of the terminal Y chalcogen species. According to TD-DFT calculations and based on experimental widths at half heights, all neutral species show very large molar extinction coefficients ε (the largest being calculated for **6**), while monoanions feature ε values that are about 40% of those calculated for the corresponding neutral species (Table S17, ESI†).

Since electrochemical measurements could not be recorded, one-electron absolute reduction potentials at 298 K were calculated from DFT thermochemical data and the corresponding values referred to the F_c^+/F_c couple in CH_2Cl_2 solution ($E_{1/2}^{298K}$) were evaluated by adopting a corrected scaling scheme (Table 1 and Table S18 in the ESI†).[36,37] Although the calculated $E_{1/2}^{298K}$ values should be considered as mere estimates, nonetheless they show that the stability of the neutral species with respect to monoanions depends on the interplay of the central metal ions and the X/Y chalcogen species. In general, Pt complexes show reduction potentials more negative than those of the corresponding Ni species, while the $E_{1/2}^{298K}$ values tend to become less negative upon increasing the content of selenium in the complexes, confirming the more oxidizing nature of 1,2-diselenolene as compared to 1,2-dithiolene analogues for different bis(1,2-dichalcogenolene) Ni, Pd, and Pt complexes.[38] As a consequence, the species showing the most negative reduction potential is **2**, while the least negative values were calculated for **7** and **8**, in perfect agreement with the experimental NIR absorption spectra recorded on the products of the syntheses, which only showed the absorption band characteristic of the neutral species for **2**, and those peculiar to monoanions for **7** and **8** (Table 1).

In conclusion, the first examples of the Ni and Pt members of three new families of bis(1,2-dichalcogenolene) complexes have been prepared and their electronic features have been investigated by means of a combined spectroscopic and theoretical investigation. Both the ability of these complexes to reversibly carry different charges and the characteristic electrochromic absorption in the NIR region are related to the composition of the nature of the frontier molecular orbitals. In particular, the minor contributions from the *n*d atomic orbitals of the metal ions to the LUMO differentiate systematically the complexes of the two metals, while selenium replacing sulfur induces a stabilization of the HOMO of the monoanions $\mathbf{1}^-$–$\mathbf{8}^-$, thus determining the blue shift observed experimentally for the π–π* NIR transition. Therefore, the choice of the central metal ion and the chalcogen atoms X and Y allows tailoring of the NIR optical properties of the resulting compounds and the relative stabilities of the neutral and monoanionic species. In analogy to what previously found for $[M(R_2timdt)_2]^{0/-}$ complexes, the overall insight into the electrochemical and NIR spectroscopic features of complexes reported here opens the way to the investigation of $[M(R_2simdt)_2]^{0/-}$, $[M(R_2timds)_2]^{0/-}$ and $[M(R_2simds)_2]^{0/-}$ 1,2-dithiolenes and 1,2-diselenolenes as active materials in devices of interest in optical processing and NIR photoconducting devices. An extended synthetic program is ongoing in our laboratory with the aim to verify the effect of the variation of the *N*-substituents on the stability of the complexes, aimed to experimentally characterize their spectroelectrochemical features in solution.

Experimental

The details of materials and methods, X-ray diffraction analyses and theoretical calculations are provided in the ESI.†

Synthesis of complexes 1–8

4.0 mmol of 1,3-dimethylimidazole-2-thione (0.50 g, for **1**, **2**, **5** and **6**) or 2-selone (0.69 g for **3**, **4**, **7** and **8**) were dissolved under N_2 in 15 mL of freshly distilled THF and cooled to −10 °C in a liquid N_2/ethylene glycol bath. LDA (THF solution 0.26 M, 15 mL, 4.0 mmol) was added dropwise and the reaction mixture was left under stirring for 30 minutes. 5.0 mmol of S (0.17 g for complexes **1–4**) or Se (0.39 g for complexes **5–8**) were added and, after further 30 minutes, 20 mL of the LDA solution (5.2 mmol) were added. After 3 h, a second aliquot (7.0 mmol) of elemental chalcogen was added (0.22 and 0.55 g of elemental sulfur and selenium, respectively), followed by 1.9 mmol of the

relevant metal salt ($NiCl_2 \cdot 6H_2O$, 0.45 g, in the case of complexes **1**, **3**, **5**, and **7**; and K_2PtCl_4, 0.79 g, in the case of **2**, **4**, **6**, and **8**) and 3.9 mmol (0.98 g) of Et_4NI. After 24 h, the solid was filtered, washed with ethyl ether and dried under vacuum and stored under an Ar atmosphere [1.22, 1.29, 0.56, 0.83, 1.98, 1.61, 1.88, and 1.53 g for $Et_4N(\mathbf{1}^-)$/**1**, $Et_4N(\mathbf{2}^-)$/**2**, $Et_4N(\mathbf{3}^-)$/**3**, $Et_4N(\mathbf{4}^-)$/**4**, $Et_4N(\mathbf{5}^-)$/**5**, $Et_4N(\mathbf{6}^-)$/**6**, $Et_4N(\mathbf{7}^-)$/**7**, and $Et_4N(\mathbf{8}^-)$/**8**, respectively].

Synthesis of complex 9

A suspension of 1,3-diethyl-2-thioxoimidazolidine-4,5-dione (0.50 g, 2.68 mmol), LR (1.50 g, 3.7 mmol), and $PtCl_2$ (0.35 g, 1.31 mmol) was refluxed under a dry N_2 atmosphere for 45 minutes. The reaction mixture was concentrated and poured into CH_3OH (30 mL). The solid was filtered and re-crystallized from CH_2Cl_2/CH_3OH solution. Yield 19%. M.p. > 210 °C. After cooling, single crystals, suitable for the X-ray diffraction analysis, were filtered off, washed with hexane, and dried under vacuum.

Elemental analyses, FT-IR spectra, m.p. for **1–9**, and CV data for **9** are provided in the ESI.†

Acknowledgements

Dipartimento di Scienze Chimiche e Geologiche of the Università degli Studi di Cagliari and Fondazione di Sardegna, Italy, are kindly acknowledged for financial support (PRID 2015).

Notes and references

‡ NIR spectra were recorded on $CHCl_3$, MeCN, THF, and DMF solutions (Table S2 in the ESI†), showing only modest variations for the explored solvents with the only exception of MeCN, whose solutions sport a systematic hypsochromic shift $\Delta\lambda_{solv}$ in the NIR absorption of both neutral and monoanionic species ($\Delta\lambda_{solv}$ in the range of 10–30 and 10–60 nm for neutral and monoanionic species, respectively, as compared to CH_2Cl_2 absorption wavelengths). IEF-PCM TD-DFT calculations (Table S16, ESI†) confirm the systematic redshift of the NIR absorption in MeCN solution.

§ The crystal structure of **9**, isostructural with $[Pd(Et_2timdt)_2]$,[39] adopts an idealized C_{2h} symmetry, and shows the metal ion in a crystallographic inversion center with a square-planar coordination. Discrete molecular units, planar but for the ethyl substituents, are stacked along the *b* direction (Fig. S6 in the ESI†), each metal ion being ''sandwiched'' between pairs of imidazolidine rings of parallel adjacent molecules. The stacks feature very weak S3···S3e and S3···S3f contacts between the terminal chalcogen atoms (3.592 Å; *e* = 5/2 − *x*, −1/2 + *y*, 1/2 − *z*; *f* = 5/2 − *x*, 1/2 + *y*, 1/2 − *z*; Table S11 in the ESI†).

¶ Neutral bis(1,2-dithiolene) complexes ML_2 have been reported to have a remarkable single diradical contribution $[M(L)_2]$ to the GS.[40,41] Therefore, the stability of the DFT wavefunctions was investigated for complexes $[M(Me_2timdt)_2]$, revealing a restricted/unrestricted instability for neutral species, the energy difference between the closed shell singlet and the diradical singlet GS configurations being 1747 and 1168 cm^{-1} for **1** and **2**, respectively. A broken-symmetry optimization of the wavefunction allowed modeling the singlet diradical description for **1–8**. Within this approach the NIR absorption assumes a ligand-to-ligand charge transfer (LLCT) character (Fig. S11 in the ESI†). This notwithstanding, when adopting the optimized wavefunction for geometry optimizations, a decrease in the agreement between calculated and structural metric parameters and an overestimation of NIR absorption energies were found (M–S = 2.193 and 2.221 Å for **1**; 2.307 and 2.326 Å for **2** within a restricted and diradical approach, respectively; NIR excitation energy 1.372 and 1.527 eV for **1**; 1.389 and 1.478 eV for **2** within a restricted and diradical approach, respectively), even when solvation was taken into account (excitation energy for the diradical of **1** in CH_2Cl_2 1.462 eV). This suggested that the contribution of the diradical singlet configuration to the GS for the complexes deriving from 2-chalcogenoxo-1,3-imidazoline-4,5-dichalcogenolato ligands might be minor. Therefore, the restricted approach was preferred in this work for neutral complexes **1–8**, which eventually led to correct bond distances and no negative excitation energies.

1 A. Zarkadoulas, E. Koutsouri and C. A. Mitsopoulou, *Coord. Chem. Rev.*, 2012, **256**, 2424–2434.
2 B. Garreau-de Bonneval, K. I. Moineau-Chane Ching, F. Alary, T.-T. Bui and L. Valade, *Coord. Chem. Rev.*, 2010, **254**, 1457–1467.
3 M. Arca, M. C. Aragoni and A. Pintus, 1,2-dichalcogenolene ligands and related metal complexes, in *Handbook of chalcogen chemistry*, ed. F. A. Devillanova and W.-W. du Mont, RSC Publishing, Cambridge, UK, 2013, ch. 11.3.
4 P. Deplano, L. Pilia, D. Espa, M. L. Mercuri and A. Serpe, *Coord. Chem. Rev.*, 2010, **254**, 1434–1447.
5 G. Chatzikyriakos, I. Papagiannouli, S. Couris, G. C. Anyfantis and G. C. Papavassiliou, *Chem. Phys. Lett.*, 2011, **513**, 229–235.
6 Y. Liu, Z. Zhang, X. Chen, S. Xu and S. Cao, *Dyes Pigm.*, 2016, **128**, 179–189.
7 Y. Le Gal, A. Vacher, V. Dorcet, M. Fourmigué, J. Crassous and D. Lorcy, *New J. Chem.*, 2015, **39**, 122–129.
8 W. F. Guo, X. B. Sun, J. Sun, X. Q. Wang, G. H. Zhang, Q. Ren and D. Xu, *Chem. Phys. Lett.*, 2007, **435**, 65–68.
9 T. Cassano, R. Tommasi, L. Nitti, M. C. Aragoni, M. Arca, C. Denotti, F. A. Devillanova, F. Isaia, V. Lippolis, F. Lelj and P. Romaniello, *J. Chem. Phys.*, 2003, **118**, 5995–6002.
10 T. Higashino, O. Jeannin, T. Kawamoto, D. Lorcy, T. Mori and M. Fourmigué, *Inorg. Chem.*, 2015, **54**, 9908–9913.
11 T. Kambe, R. Sakamoto, T. Kusamoto, T. Pal, N. Fukui, K. Hoshiko, T. Shimojima, Z. Wang, T. Hirahara, K. Ishizaka, S. Hasegawa, F. Liu and H. Nishihara, *J. Am. Chem. Soc.*, 2014, **136**, 14357–14360.
12 A. Kobayashi, H. Kim, Y. Sasaki, R. Kato and H. Kobayashi, *Solid State Commun.*, 1987, **62**, 57–64.
13 R. Kato, *Chem. Rev.*, 2004, **104**, 5319–5346.
14 J.-P. Porcher, T. Fogeron, M. Gomez-Mingot, L.-M. Chamoreau, Y. Li and M. Fontecave, *Chem. – Eur. J.*, 2016, **22**, 4447–4453.
15 D. K. Dhaked and P. V. Bharatam, *J. Inorg. Biochem.*, 2015, **142**, 84–91.
16 H. Sugimoto, H. Tano, K. Toyota, R. Tajima, H. Miyake, I. Takahashi, S. Hirota and S. Itoh, *J. Am. Chem. Soc.*, 2010, **132**, 8–9.
17 J. McMaster, J. M. Tunney and C. D. Garner, *Prog. Inorg. Chem.*, 2004, **52**, 539–583.
18 R. Eisemberg and H. B. Gray, *Inorg. Chem.*, 2011, **50**, 9741–9751.
19 M. C. Aragoni, M. Arca, F. Demartin, F. A. Devillanova, A. Garau, F. Isaia, F. Lelj, V. Lippolis and G. Verani, *J. Am. Chem. Soc.*, 1999, **121**, 7098–7107.
20 P. Romaniello and F. Lelj, *J. Phys. Lett.*, 2003, **372**, 51–58.
21 T. Cassano, R. Tommasi, M. Arca and F. A. Devillanova, *J. Phys.: Condens. Matter*, 2006, **18**, 5279–5290.
22 M. C. Aragoni, M. Arca, M. Caironi, C. Denotti, F. A. Devillanova, E. Grigiotti, F. Isaia, F. Laschi, V. Lippolis, D. Natali, L. Pala, M. Sampietro and P. Zanello, *Chem. Commun.*, 2004, 1882–1883.

23 T. Agostinelli, M. Caironi, D. Natali, M. Sampietro, M. Arca, F. A. Devillanova and F. A. Ferrero, *Synth. Met.*, 2007, **157**, 984–987.
24 K. Mebrouk, F. Camerel, O. Jeannin, B. Heinrich, B. Donnio and M. Fourmigué, *Inorg. Chem.*, 2016, **55**, 1296–1303.
25 M. C. Aragoni, M. Arca, T. Cassano, C. Denotti, F. A. Devillanova, R. Frau, F. Isaia, F. Lelj, V. Lippolis, L. Nitti, P. Romaniello, R. Tommasi and G. Verani, *Eur. J. Inorg. Chem.*, 2003, 1939–1947.
26 See for example: (*a*) A. L. Gushchin, R. Llusar, C. Vicent, P. A. Abramov and C. J. Gómez-Garcia, *Eur. J. Inorg. Chem.*, 2013, 2615–2622; (*b*) G. Yzambart, N. Bellec, G. Nasser, O. Jeannin, T. Roisnel, M. Fourmigué, P. Auban-Senzier, J. Íñiguez, E. Canadell and D. Lorcy, *J. Am. Chem. Soc.*, 2012, **134**, 17138–17148; (*c*) C. P. Morley, C. A. Webster, P. Douglas, K. Rofe and M. Di Vaira, *Dalton Trans.*, 2010, 3177–3189.
27 M. C. Aragoni, M. Arca, F. A. Devillanova, F. Isaia, V. Lippolis, A. Mancini, L. Pala, A. M. Z. Slawin and J. D. Woollins, *Inorg. Chem.*, 2005, **44**, 9610–9612.
28 S. Eid, M. Fourmigué, T. Roisnel and D. Lorcy, *Inorg. Chem.*, 2007, **46**, 10647–10654.
29 P. Romaniello and F. Lelj, *THEOCHEM*, 2003, **636**, 23–37.
30 B. S. Pedersen, S. Scheibye, N. H. Nilsson and S.-O. Lawesson, *Bull. Soc. Chim. Belg.*, 1978, **87**, 223–228.
31 M. Arca, F. Demartin, F. A. Devillanova, F. Isaia, F. Lelj, V. Lippolis and G. Verani, *Can. J. Chem.*, 2000, **78**, 1147–1157.
32 I. P. Gray, P. Bhattacharyya, A. M. Z. Slawin and J. D. Woollins, *Chem. – Eur. J.*, 2005, **11**, 6221–6227.
33 B. L. Benac, E. M. Burgess and A. J. Arduengo III, *J. Org. Synth. Coll.*, 1986, **64**, 92–95.
34 D. J. Williams, M. R. Fawcett-Brown, R. R. Raye, D. VanDerveer, Y. T. Pang, R. L. Jones and K. L. Bergbauer, *Heteroat. Chem.*, 1993, **4**, 409–413.
35 W. Koch and M. C. Holthausen, *A Chemist's Guide to Density Functional Theory*, Wiley-VCH, Weinheim, 2nd edn, 2002.
36 A. P. Davis and A. J. Fry, *J. Phys. Chem. A*, 2010, **114**, 12299–12304.
37 V. T. T. Huong, T. B. Tai and M. T. Nguyen, *Phys. Chem. Chem. Phys.*, 2016, **18**, 6259–6267.
38 E. A. C. Bushnell and R. J. Boyd, *Int. J. Quantum Chem.*, 2016, **116**, 369–376.
39 M. Arca, F. Demartin, F. A. Devillanova, A. Garau, F. Isaia, F. Lelj, V. Lippolis, S. Pedraglio and G. Verani, *J. Chem. Soc., Dalton Trans.*, 1998, 3731–3736.
40 S. Sproules and K. Wieghardt, *Coord. Chem. Rev.*, 2011, **255**, 837–860.
41 K. Ray, T. Weyhermüller, F. Neese and K. Wieghardt, *Inorg. Chem.*, 2005, **44**, 5345–5360.

